JOC The Journal of Organic Chemistry

Article

pubs.acs.org/joc

Synthesis and Structural Characterization of a TCNQ Based Organic Semi-Conducting Material with a 2:5 Stoichiometry

Jinzhen Lu,[†] Xiaohu Qu,[†] Germanas Peleckis,[§] John F Boas,[‡] Alan M Bond,*[,†] and Lisandra L Martin*[,†]

[†]School of Chemistry and [‡]School of Physics, Monash University, Clayton, VIC 3800, Australia

[§]Institute for Superconducting and Electronic Materials Faculty of Engineering, The University of Wollongong, Wollongong, NSW 2522, Australia

Supporting Information

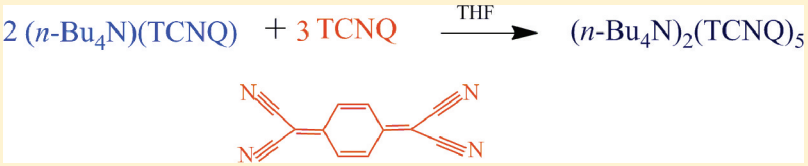

ABSTRACT: The tetrabutylammonium complex with a 2:5 stoichiometry, $(n\text{-}Bu_4N)_2(TCNQ)_5$, has been prepared and structurally characterized by X-ray crystallography. Diagnostic bands in the Raman spectrum and signature features in the electrochemistry confirm that the TCNQ moieties are partially charged in the solid state. EPR, magnetic susceptibility, and electrical conductivity measurements are all consistent with $(n\text{-}Bu_4N)_2(TCNQ)_5$ behaving as a quasi-one-dimensional organic semiconductor.

INTRODUCTION

7,7′,8,8′-Tetracyanoquinodimethane (TCNQ) is well-known to be an electron acceptor which readily forms charge−transfer (CT) complexes.[1,2,3] These TCNQ-based materials are found with a number of different cation:anion stoichiometries and are of considerable interest because of their extensive and novel electrical, electrochemical, and magnetic properties arising from the characteristic π-stacking of the TCNQ moieties into columns. Accordingly they offer exciting applications as molecular devices.[4,5−15]

TCNQ derivatives with lower stoichiometries are quite common and generally exhibit weak semiconductivity at room temperature,[3,16−23] although (TTF)(TCNQ) is a rare case of an organic metal conductor.[24] Examples with higher stoichiometries are rare and were reported by Ashwell et al. ~30 years ago. These included 2:5,[25] 1:4,[26−29] and 1:5[30,31] cation:anion ratios, and these complexes all employed bipyridinium dication derivatives. These examples display the high range semiconductivity (2×10^{-3} to 2.2×10^{3} S cm^{-1}), and one even shows metallic behavior at low temperature.[32] Interestingly, X-ray structures of these higher stoichiometries reveal that the TCNQ moieties are arranged into tetramers or pentamers, suggesting that these small organisational units within the TCNQ column enhance the conductivity for these samples.[25−31]

Of the TCNQ complexes in which the cations are tetraalkylammonium salts (e.g., Me_4N, Et_4N, Pr_4N, and Bu_4N), the highest stoichiometry reported to date is 2:3,[33] and only a 1:1 complex has been crystallized for the tetrabutylammonium-TCNQ case.[34] Here we report the synthesis, the single crystal X-ray structure, and comprehensive physicochemical characterization of a new tetrabutylammonium−TCNQ complex with the unusual higher stoichiometry of 2:5.

RESULTS AND DISCUSSION

The complex was synthesized by mixing 0.3 mM equivalence of $(n\text{-}Bu_4N)(TCNQ)$ and $TCNQ^0$ in THF. The solution was filtered to remove some precipitants followed by evaporation of the solvent to afford a dark blue solid. Single crystals were grown by diffusion of diethyl ether into a methanol solution and were suitable for X-ray crystallographic studies. The polycrystalline solid was also characterized by NMR, IR, and Raman spectroscopy and electrochemistry. These data supported the formulation $(n\text{-}Bu_4N)_2(TCNQ)_5 \cdot 2MeOH$ and are consistent with the single crystal structure.

The complex crystallized in the triclinic space group *P*-1. The asymmetric unit contained one $n\text{-}Bu_4N$ cation with its charge balanced by the two and a half TCNQ species. One methanol solvent of crystallization was also included (Supporting Information Figure S1). The crystal structure shown in Figure 1A reveals that the TCNQ columns are separated by the $n\text{-}Bu_4N$ cation layers, resulting in a 2D network supported by weak hydrogen bonding between the nitrile groups of the TCNQ's and the CH_2 groups of the $n\text{-}Bu_4N$ cations. The methanol solvate is clearly resolved and resides between the TCNQ columns and the $n\text{-}Bu_4N$ cation layers as shown in Figure 1A.

The three crystallographically inequivalent TCNQ moieties, namely, TCNQ-A, TCNQ-B, and TCNQ-C, are close to planar and stack into a pentamer within the TCNQ columns,

Received: September 19, 2011
Published: November 9, 2011

   dx.doi.org/10.1021/jo2018334 | J. Org. Chem. 2011, 76, 10078−10082

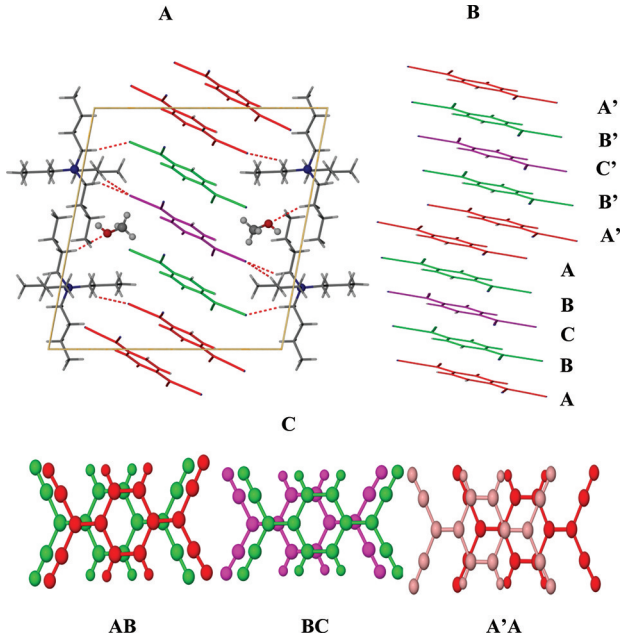

Figure 1. X-ray crystal structure of $(n\text{-}Bu_4N)_2(TCNQ)_5$. (A) The packing diagram viewed along the *c* axis illustrating columns of cation and anion. (B) The TCNQ anion stacking of the pentamers composed of individual TCNQ units (A, B and C). (C) The π-stacking of the adjacent TCNQ moieties that overlap as shown in the diagram as top-bottom: TCNQ-AB, TCNQ-BC, TCNQ-A'A.

therefore forming the ABCBAA' pattern along the *c* axis (Figure 1B). There are strong $\pi-\pi$ interactions between the adjacent TCNQ moieties, with interplanar distances of 3.22 Å (TCNQ-AB), 3.24 Å (TCNQ-BC), and 3.37 Å (TCNQ-AA'). The TCNQ moieties overlap in a pattern that is characteristic of most mixed-valence TCNQ dimers, in which the ring of one TCNQ molecule overlaps with the external double bond of a second TCNQ (Figure 1C).[16,35] However, an interesting structural feature is that the TCNQ pentamers are also offset or staggered along the longitudinal axis. Thus, within a TCNQ pentamer, the external bond to ring overlap for adjacent TCNQ's is in the same direction (Figure 1C, TCNQ-AB, TCNQ-BC); however, between pentamers the direction for "staggering" is reversed (Figure 1C, TCNQ-A'A). We speculate that such ordering may result in the somewhat lower conductivity observed in our case in comparison with the published examples containing $(cation)_n:(TCNQ)_5$ ratio complexes (n = 1, 2).[25,30] The degree of charge transfer (ρ) for $(n\text{-}Bu_4N)_2(TCNQ)_5$ can be estimated using an empirical relationship correlating the bond lengths of each TCNQ moiety.[36,37] We calculate these ρ values to be −0.3 (TCNQ-A), −0.5 (TCNQ-B), and −0.4 (TCNQ-C). Interestingly, the two electrons are unevenly distributed over the TCNQ pentamers. Thus the total charge across the five TCNQ moieties can be estimated as ca. −2.0 as required for neutralization of the two cations. This is in marked contrast to the bipyridinium−TCNQ complexes, in which we have calculated ρ and shown that the charges are evenly distributed across the TCNQ pentamer for the 2:5 complex,[25] and also in the case of the 1:5 complex,[31] the one charge is localized on 2 of the 5 TCNQ moieties and the remaining TCNQ moieties are approximately neutral.

Raman and IR spectroscopy were also used to support the analysis for the degree of charge transfer for the TCNQ moieties. In the Raman spectrum, two stretching bands at 2211 and 1437 cm^{-1}, corresponding to the C≡N and the extracyclic C═C groups, were observed. These frequencies lie between those expected for the neutral TCNQ and anionic $TCNQ^{1-}$,[16] indicative of a partially charged TCNQ moiety in the solid state. The IR spectrum confirmed that the complex contained fractionally charged TCNQ species with sharp stretching bands at 2197 and 2160 cm^{-1} attributable to C≡N, strong absorption of C−H band at 834 cm^{-1}, again lying between that expected for $TCNQ^0$ and $TCNQ^{1-}$.

In the solution phase, the TCNQ pentamer is believed to dissociate into $TCNQ^0$ and $TCNQ^{1-}$. Electrochemical studies of TCNQ are characterized by two well-defined $TCNQ^{0/1-}$ and $TCNQ^{1-/2-}$ reduction processes in acetonitrile (0.1 M Bu_4NPF_6). Steady-state voltammetry is a useful method to determine the redox level of the species, from the position of zero current. Thus the steady-state voltammogram shown in Figure 2 (black curve) has the zero current passing through the

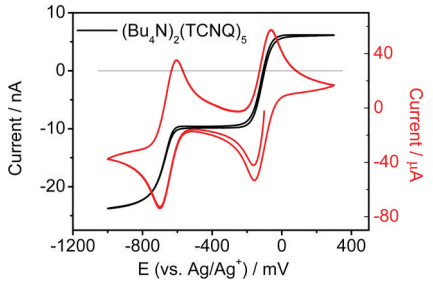

Figure 2. Steady-state (black curve) and transient voltammograms (red curve) of a 1.0 mM $(n\text{-}Bu_4N)_2(TCNQ)_5$ MeCN solution containing 0.1 M Bu_4NPF_6 as the supporting electrolyte. Steady-state employed a 10 μm diameter Pt electrode at a scan rate of 50 mV s^{-1}. Cyclic voltammogram (red curve) employed a 2.0 mm diameter glassy carbon electrode at a scan rate of 100 mV s^{-1}.

first reduction process $TCNQ^{0/1-}$ at a level that corresponds to 39% $TCNQ^{1-}$ and 61% $TCNQ^0$ and is close to the value of 2 $TCNQ^{1-}$ per 3 $TCNQ^0$. Once again, this agrees well with the stoichiometry deduced from crystal structure. A UV−vis study in acetonitrile (Supporting Information, Figure S2) also supports the coexistence of $TCNQ^0$ and $TCNQ^{1-}$ in solution at a ratio of close to 2:3. Thus both electrochemical and UV−vis studies confirm that TCNQ moieties in the solid dissociate into neutral $TCNQ^0$ and $TCNQ^{1-}$ in acetonitrile. This pseudo-disproportionation has been observed previously for the $(n\text{-}Pr_4N)(TCNQ)_2$ solid.[22]

Room temperature electrical conductivity (S) measurements were obtained using a pressed pellet and gave $S_{(RT)}$ = 7.1 × 10^{-3} S cm^{-1}. This is within the typical semiconductor range. The temperature dependence of the resistance was obtained using a single crystal with a four point probe, which also confirmed the semiconducting behavior, as shown in Figure 3. The absolute value of resistance (R) at room temperature was 24 kΩ. The electrical resistance of several single crystals was measured between 300 and ∼200 K, and these samples all showed an exponential increase in electrical resistance with decreasing temperature. A further decrease in temperature caused a dramatic increase in R to values that were beyond the experimental range of the equipment used. This temperature dependence is characteristic of a Type I semiconductor[38,39] and can be represented by an equation of the form $R = R_0\, e^{E/KT}$, where E is an activation energy and T is the absolute temperature. The data in Figure 3 gives an estimate for E of

dx.doi.org/10.1021/jo2018334 | J. Org. Chem. 2011, 76, 10078−10082

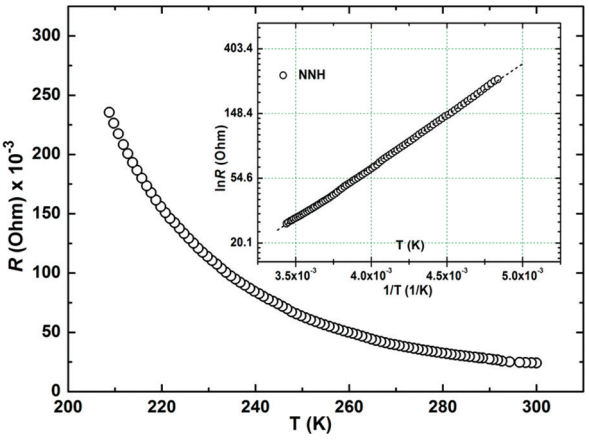

Figure 3. The temperature dependence of the resistance of a single crystal of $(n\text{-}Bu_4N)_2(TCNQ)_5$. The inset figure shows the data fitted according to the nearest neighbor hopping transport model. (○) Experimental data.

~0.15 eV. However, a detailed exposition of the conduction mechanism (i.e., whether nearest neighbor hopping is used to fit the data, see insert in Figure 3, or a band gap model that also can be used to fit the data, not shown) awaits further study. Due to fragility and small size of the single crystals, it was impossible to measure the resistance along a particular crystal direction, e.g., along the axis of the TCNQ pentamer columns. Thus it is not surprising that the conductivity we report here was somewhat lower than we anticipitated, and we noted that it was also lower than that of some of the other TCNQ pentamer complexes.[25,29,30,32]

The EPR spectrum of a polycrystalline powder of $(n\text{-}Bu_4N)_2(TCNQ)_5$ exhibited an intense resonance at 290 K with partially resolved orthorhombic features with g_1 = 2.0037, g_2 = 2.0029, and g_3 = 2.0025 (Figure 4a). These g-values are typical

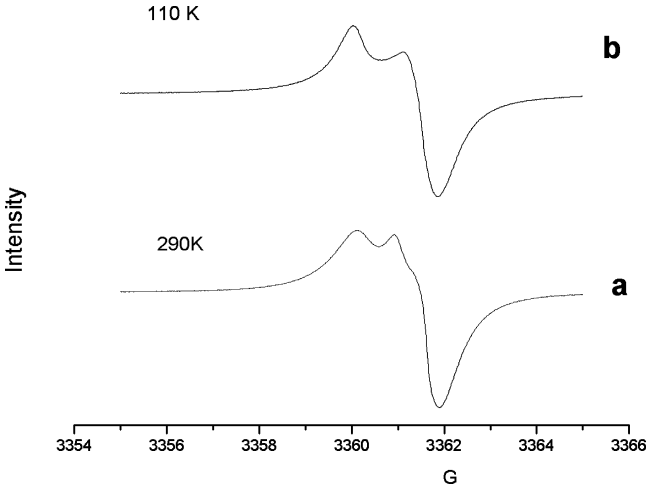

Figure 4. EPR spectra of a polycrystalline powder of $(n\text{-}Bu_4N)_2(TCNQ)_5$ at (a) 290 K and 9.4228 GHz and (b) 110 K and 9.4215 GHz. Spectrometer settings: microwave power 1.05 μW; 100 kHz modulation amplitude 10 μT; field scan range/time 1 mT/41.9 s; time constant 20.48 ms; spectrometer gains (a) 1.0×10^3 and (b) 2.0×10^2.

for $TCNQ^{1-}$ anions[40] and are very similar to those found for $(n\text{-}Pr_4N)(TCNQ)_2$.[22] As also was the case for $(n\text{-}Pr_4N)(TCNQ)_2$, a reduction in temperature to 110 K resulted in a spectrum with the appearance of axial symmetry with $g_\parallel$ = 2.0034 and $g_\perp$ = 2.0024 (Figure 4b). The lowering of the temperature to 110 K resulted in a decrease in the product $I \times T$ to about two-thirds of its value at 290 K, where I is the area under the absorption curve, T is the temperature and the product $I \times T$ is proportional to the effective number of unpaired spins with S = 1/2. This decrease is consistent with the magnetic susceptibility measurements described below and is indicative of antiferromagnetic interactions between the electron spins. However, the absence of EPR resonances in the regions around g = 2 and g = 4, even at system gains 10^5 times higher than that used for Figure 4, indicates that the two electrons per $(n\text{-}Bu_4N)_2(TCNQ)_5$ unit do not form a discrete antiferromagnetically coupled pair with spin S =1 similar to that found for $(n\text{-}Pr_4N)(TCNQ)$.[22] Rather, the electrons are delocalized over the TCNQ chain and are sufficiently mobile on the EPR time scale (~10^{-10} s) for both the electron–nuclear hyperfine interactions and the dipolar interactions between nearby spins to be averaged out.[22]

The temperature dependence of the static magnetic susceptibility of a polycrystalline powder of $(n\text{-}Bu_4N)_2(TCNQ)_5$ (Figure 5) shows a maximum in the curve

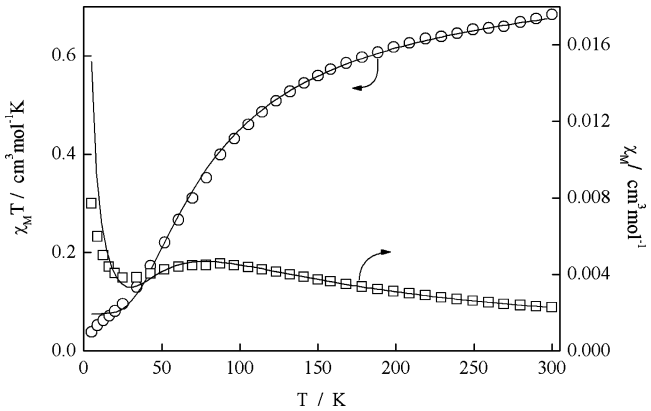

Figure 5. Plot of temperature dependence of the magnetic susceptibility χ_M (□) and $\chi_M T$ (○) for $(n\text{-}Bu_4N)_2(TCNQ)_5$ measured at 0.5 T magnetic field.

at ~80 K and a paramagnetic Curie-like tail, attributed to isolated and localized spins, below ~30 K. The μ_{eff} at 290 K corresponds to approximately two unpaired electrons per $(n\text{-}Bu_4N)_2(TCNQ)_5$ unit, consistent with the EPR intensity. The product $\chi_M T$ ($\chi_M T$ is proportional to the magnetic moment and thus the number of available spins) as a function of T shows a decrease with temperature, indicating antiferromagnetic coupling between spins. Although the temperature dependence of the magnetism between 300 and ~20 K can be fitted to a dimer model with two electrons per $(n\text{-}Bu_4N)_2(TCNQ)_5$ unit and an antiferromagnetic exchange interaction J = −54 cm^{-1}, the results are better described as being due to a quasi-one-dimensional Heisenberg antiferromagnetic system.[41,42] A description of the present system in these terms is also consistent with the resistance and EPR measurements. The similarity of the temperature dependence of both χ_M and $\chi_M T$ of $(n\text{-}Bu_4N)_2(TCNQ)_5$ with that of the quasi-one-dimensional organic semiconductor $(n\text{-}Bu_2NH_2)(TCNQ)_2$[43] should be noted, although in the present case there is no clear evidence for a Peierls-like phase transition.

dx.doi.org/10.1021/jo2018334 | J. Org. Chem. 2011, 76, 10078–10082

CONCLUSIONS

In summary we have reported the synthesis of an unusually high stoichiometry organic semiconducting material, $(n\text{-}Bu_4N)_2(TCNQ)_5$, which represents the first 2:5 ratio complex found in the tetraalkylammonium−TCNQ series and is a rare example of this stoichiometry. X-ray structure analyses indicated that the complex consists of a layered structure supported by H-bond interactions. The TCNQ anions form a 1D pentamer column with a short interplanar distances of 3.2 Å, leading to a comparatively high conductivity. Raman and IR spectroscopy support partially charged TCNQ moieties in the solid state. The solution studies by electrochemistry and UV−vis spectrum indicated that $(n\text{-}Bu_4N)_2(TCNQ)_5$ complex undergoes a pseudo-disproportionation into $TCNQ^0$ and $TCNQ^{1-}$ in MeCN. Both the magnetic susceptibility and EPR spectra of this new material showed behavior typical of a quasi-one-dimensional organic semiconductor.

EXPERIMENTAL SECTION

Chemicals. Tetrabutylammonium bromide, tetrabutylammonium iodide, lithium iodide, methanol, acetone, acetonitrile, tetrahydrofuran, diethyl ether were used as received. 7,7′,8,8′-Tetracyanoquinodimethane (TCNQ) was recrystallized from acetonitrile prior to use. Tetrabutylammonium hexafluorophosphate was recrystallized twice from ethanol before use. Gold-coated glass slides with a typical area of 0.20 cm^2 were used as substrates for Raman characterizations. All aqueous solutions were prepared from water of resistivity of 18.2 MΩ·cm.

Synthesis of the Title Complex, $(n\text{-}Bu_4N)_2(TCNQ)_5$. $(n\text{-}Bu_4N)(TCNQ)$ (141 mg, 0.31 mmol) in THF (5 mL) and 64.2 mg (0.31 mmol) of $TCNQ^0$ in THF (5 mL) were combined and stirred for 2 h under N_2 at room temperature. After filtration, the solvent was removed via rotary evaporation, yielding dark blue powders [120 mg, 51% based on $(n\text{-}Bu_4N)(TCNQ)$]. ^1H NMR (300 MHz, methanol-d_4): δ 1.05 (t, J = 6.6 Hz, 13.2), 1.45 (m) 1.69 (m), 3.23 (m). FT-IR (ν/cm^{-1}): 2197(s), 2160(bs), 1563(s), 1529(m), 1473(w), 1426(s), 1305(s), 1106(s), 1069(s), 951(s), 888(m), 834(s), 742(w), 736(w), 692(s). Anal. Calcd for $(Bu_4N)(TCNQ)_{2.5}$.MeOH [$C_{47}H_{50}N_{11}O$]: C, 71.94, H 6.38, N, 19.64. Found: C, 72.17, H 6.66, N, 19.92.

Single crystals suitable for X-ray analysis were obtained by diffusion of diethyl ether into a methanolic solution of the complex over two weeks. Crystal data for $C_{47}H_{46}N_{11}O$, M = 780.95, 0.30 × 0.16 × 0.12 mm^3, triclinic, space group P-1 (No. 2), a = 7.7869(6), b = 16.4712(12), c = 17.3078(13) Å, α = 100.676(4)°, β = 92.585(4)°, γ = 92.799(4)°, V = 2175.5(3) $Å^3$, Z = 2, D_c = 1.192 g/cm^3, F_{000} = 826, Mo Kα radiation, λ = 0.71073 Å, T = 123(2) K, $2\theta_{max}$ = 50.0°, 27917 reflections collected, 7505 unique (R_{int} = 0.0560). Final GoF = 1.022, $R1$ = 0.0666, $wR2$ = 0.1765, R indices based on 4546 reflections with $I > 2\sigma(I)$ (refinement on F^2), 538 parameters, 0 restraints. Lp and absorption corrections applied, μ = 0.075 mm^{-1}. The asymmetric unit of the single crystal is shown in Supporting Information, Figure S1.

Electrochemical Procedures and Instrumentation. Voltammetric experiments were conducted with an electrochemical workstation at room temperature (22 ± 2 °C). Either a 2.0 mm diameter glassy carbon macrodisk electrode (area = 0.0297 cm^2) or Pt microelectrode (diameter = 10 μm) was used as the working electrode. The Pt counter electrode was placed directly in the test solution and an Ag/Ag^+ reference electrode (10 mM $AgNO_3$, 0.1M Bu_4NPF_6, in MeCN) was separated from the test solution by a salt bridge containing the supporting electrolyte.

Physical Characterization Procedures. A single crystal was mounted on fine glass fibres using viscous hydrocarbon oil. Data were collected using a diffractionometer equipped with graphite monochromated Mo Kα radiation. The data collection temperature was maintained at 123 K using an open-flow N_2 cryostream. The structure was solved by direct methods using SHELXS-97.[44] Least-squares refinements against F^2 were carried out using SHELXL-97 with the program X-Seed as a graphical interface.[45] All non-hydrogen atoms were anisotropically refined, and all hydrogen atoms were placed in their calculated positions and refined following the riding model. CCDC 817922 contains the supplementary crystallographic data for this paper and can be obtained free of charge from the Cambridge Crystallographic Data Centre via www.ccdc.cam.ac.uk/data_request/cif. XRD powder diffraction was measured with a diffractionmeter with Cu Kα radiation (λ = 1.5418 Å). An aluminum insert was used due to limited sample size.

Raman spectra were acquired with a spectrometer and microscope using a 514 nm laser line and a power of 18mW. FT-IR spectra were recorded using an ATR Instrument. ^1H NMR spectra were obtained using an 300 MHz spectrometer. ^1H resonances were referenced to residual hydrogen from methanol-d_4 as 3.31 ppm (vs TMS).

X-band (ca. 9.4 GHz) EPR spectra were recorded with a spectrometer. Temperatures between 290 and 110 K were obtained using the standard rectangular TE_{102} cavity together with a temperature controller and associated nitrogen gas flow insert. The microwave frequency was measured with an Microwave 548A frequency counter, and the g-values were determined by reference to the F^+ line in CaO (g = 2.0001 ± 0.0001).[46] The experimental spectra were obtained as the first derivative of the absorption. The spectral intensities were obtained by double integration of the experimental spectrum. The g-values were estimated by spectrum simulations using a computer simulation software suite.[47] The uncertainty in the g-values is estimated as ±0.0002. Magnetic susceptibility measurements were made with sample masses of ∼30 mg using a magnetometer in a dc field of 0.5 T.

Conductivity Measurements. Room temperature conductivity measurements were carried out on a pressed pellet of the complex with a four-point probe test meter. The measurements of the conductivity on a single crystal have been done using standard four probe technique. Because of the fragile nature of the samples, first, single crystals were carefully attached to a MgO single crystalline substrate by nonconducting apiezon paste. Then the substrate was secured on the resistivity puck by double-sided sticky tape. For electrical connection, four contacts were made using high grade silver paste and 25 μm gold wires. After insertion of the resistivity puck into a chamber, it was purged with He gas and evacuated to a pressure of around 5 Torr. The resistivity versus temperature scans were done by sweeping the temperature at a rate of 3 K/min from 300 to 200 K.

ASSOCIATED CONTENT

Supporting Information

^1H NMR, UV−vis, XRD, and crystallographic information in CIF form for the complex $(n\text{-}Bu_4N)_2(TCNQ)_5$. This material is available free of charge via the Internet at http://pubs.acs.org.

AUTHOR INFORMATION

Corresponding Author

*E-mail: alan.bond@monash.edu; lisa.martin@monash.edu.

ACKNOWLEDGMENTS

The Australian Research Council is gratefully acknowledged for financial support to A.M.B. and L.L.M. We thank Dr. Boujemaa Moubaraki and Prof. Keith S. Murray for performing magnetic susceptibility measurements.

REFERENCES

(1) Acker, D. S.; Harder, R. J.; Hertler, W. R.; Mahler, W.; Melby, L. R.; Benson, R. E.; Mochel, W. E. *J. Am. Chem. Soc.* **1960**, *82*, 6408−6409.

(2) Melby, L. R.; Mahler, W.; Mochel, W. E.; Harder, R. J.; Hertler, W. R.; Benson, R. E. *J. Am. Chem. Soc.* **1962**, *84*, 3374−3387.

(3) Torrance, J. B. *Mol. Cryst. Liq. Cryst.* **1985**, *126*, 55−67.

(4) Qu, X.; Lu, J.; Zhao, C.; Boas, J. F.; Moubaraki, B.; Murray, K. S.; Siriwardana, A.; Bond, A. M.; Martin, L. L. *Angew. Chem., Int. Ed.* **2011**, *50*, 1589−1592.
(5) Bond, A. M. *Broadening Electrochemical Horizons: Principles and Illustration of Voltammetric and Related Techniques*; Oxford University Press: Oxford, 2002; Chapter 5.
(6) Kirtley, J. R.; Mannhart, J. *Nat. Mater.* **2008**, *7*, 520−521.
(7) Kivala, M.; Boudon, C.; Gisselbrecht, J. P.; Seiler, P.; Gross, M.; Diederich, F. *Chem. Commun.* **2007**, 4731−4733.
(8) Jain, R.; Kabir, K.; Gilroy, J. B.; Mitchell, K. A. R.; Wong, K. C.; Hicks, R. G. *Nature* **2007**, *445*, 291−294.
(9) Nafady, A.; Bond, A. M. *Inorg. Chem.* **2007**, *46*, 4128−4137.
(10) O'Mullane, A. P.; Neufeld, A. K.; Harris, A. R.; Bond, A. M. *Langmuir* **2006**, *22*, 10499−10505.
(11) Neufeld, A. K.; O'Mullane, A. P.; Bond, A. M. *J. Am. Chem. Soc.* **2005**, *127*, 13846−13853.
(12) Hu, Z. P.; Shen, Z. X.; Qin, L.; Tang, S. H.; Kuok, M. H.; Xu, G. Q.; Mok, K. F.; Huang, H. H. *J. Mol. Struct.* **1995**, *356*, 163−168.
(13) Wallace, W. L.; Jaeger, C. D.; Bard, A. J. *J. Am. Chem. Soc.* **1979**, *101*, 4840−4843.
(14) Mochida, T.; Yamazaki, S.; Suzuki, S.; Shimizu, S.; Mori, H. *Bull. Chem. Soc. Jpn.* **2003**, *76*, 2321−2328.
(15) Bond, A. M.; Colton, R.; van den Bergen, A.; Walter, J. N. *Organometallics* **2004**, *23*, 3164−3176.
(16) Herbstein, F. H.; Kapon, M. *Crystallogr. Rev.* **2008**, *14*, 3−74.
(17) Kuroda, N.; Sugimoto, T.; Hagiwara, M.; Hasanudin.; Ueda, K.; Tada, T.; Uozaki, H.; Toyota, N.; Mogi, I.; Watanabe, K.; Motokawa, M. *Synth. Met.* **2003**, *133*, 535−537.
(18) Andrzej, G.; Andrzej, B. *Mini-Rev. Med. Chem.* **2010**, *7*, 145−160.
(19) Chen, Y. C.; Liu, G. X.; Wang, P. F.; Xu, H.; Ren, X. M.; Song, Y.; Sui, Y. X. *Polyhedron* **2007**, *26*, 1781−1786.
(20) Chen, Y. C.; Wang, P. F.; Liu, G. X.; Xu, H.; Ren, X. M.; Song, Y.; Ni, Z. P. *J. Phys. Chem. Solids* **2008**, *69*, 2445−2452.
(21) Martin, L. L.; Siriwardana, A.; Lu, J.; Qu, X.; Zhao, C.; Bond, A. M. *Aust. J. Chem.* **2011**, *64*, 732−740.
(22) Qu, X.; Lu, J.; Boas, J. F.; Bond, A. M.; Martin, L. L. *Eur. J. chem.* **2011**, *17*, 9350−9358.
(23) Torrance, J. B. *Acc. Chem. Res.* **1979**, *12*, 79−86.
(24) Garito, A. F.; Heeger, A. J. *Acc. Chem. Res.* **1975**, *7*, 232−240.
(25) Ashwell, G. J.; Eley, D. D.; Wallwork, S. C.; Willis, M. R.; Welch, G. D.; Woodward, J. *Acta Crystallogr.* **1977**, *B33*, 2252−2257.
(26) Ashwell, G. J.; Wallwork, S. C.; Baker, S. R.; Berthier, P. I. *Acta Crystallogr.* **1975**, *B31*, 1174−1178.
(27) Ashwell, G. J.; Bartlett, V. E.; Eley, D. D.; Wallwork, S. C.; Willis, M. R. *Acta Crystallogr.* **1977**, *B33*, 2602−2607.
(28) Ashwell, G. J.; Eley, D. D.; Drew, N. J.; Wallwork, S. C.; Willis, M. R. *Acta Crystallogr.* **1977**, *B33*, 2598−2602.
(29) Ashwell, G. J.; Eley, D. D.; Fleming, R. J.; Wallwork, S. C.; Willis, M. R. *Acta Crystallogr.* **1976**, *B32*, 2948−2952.
(30) Ashwell, G. J.; Eley, D. D.; Harper, A.; Torrance, A. C.; Wallwork, S. C.; Willis, M. R. *Acta Crystallogr.* **1977**, *B33*, 2258−2263.
(31) Ashwell, G. J.; Eley, D. D.; Drew, N. J.; Wallwork, S. C.; Willis, M. R. *Acta Crystallogr.* **1978**, *B34*, 3608−3612.
(32) Ashwell, G. J.; Eley, D. D.; Willis, M. R. *Nature* **1976**, *259*, 201−202.
(33) Ueda, K.; Sugimoto, T.; Endo, S.; Toyota, N.; Kohama, M.; Yamamoto, K.; Suenaga, Y.; Morimoto, H.; Yamaguchi, T.; Munakata, M.; Hosoito, N.; Kanehisa, N.; Shibamoto, Y.; Kai, Y. *Chem. Phys. Lett.* **1996**, *261*, 295−300.
(34) O'Kane, S. A.; Clerac, R.; Zhao, H. H.; Xiang, O. Y.; Galan-Mascaros, J. R.; Heintz, R.; Dunbar, K. R. *J. Solid State Chem.* **2000**, *152*, 159−173.
(35) Herbstein, F. H. *Crystalline Molecular Complexes and Compounds*; Oxford University Press: Oxford, 2005; Vols. *1* and *2*.
(36) Flandrois, P. S.; Chasseau, D. *Acta Crystallogr., Sect. B* **1977**, *33*, 2744−2750.
(37) Kistenmacher, T. J.; Emge, T. J.; Bloch, A. N.; Cowan, D. O. *Acta Crystallogr., Sect. B* **1982**, *38*, 1193−1199.
(38) Epstein, A. J.; Conwell, E. M.; Miller, J. S. *Ann. N.Y. Acad. Sci.* **1978**, *313*, 183−209.
(39) Schwoerer, M.; Wolf, H. C. *Organic Molecular Solids*; Wiley VCH: Weiheim, 2007.
(40) Ashwell, G. L.; Jansen, S.; Jones, M. T.; Kennard, C. H. L. *Phys. Stat. Sol. A* **1983**, *80*, 127−134.
(41) Bonner, J. C.; Fisher, M. E. *Phys. Rev.* **1964**, *135A*, 640−658.
(42) Graja, A. *Low Dimensional Organic Conductors*; World Scientific: Singapore, 1992.
(43) Peng, H.; Ran, C.; Liu, Z.; Long, Y.; Wang, Z.; Yu, Z.; Sun, H.; Wei, Y.; Gao, S.; Chen, Z.; Chen, E.-Q. *J. Phys. Chem. C* **2008**, *112*, 11001−11006.
(44) Sheldrick, G. M. *Acta Crystallogr., Sect. A* **2008**, *64*, 112−122.
(45) Barbour, L. J. *J. Supramol. Chem* **2001**, *1*, 189.
(46) Wertz, J. E.; Orton, J. W.; Auzins, P. *Disc. Faraday Soc.* **1961**, *31*, 140−150.
(47) Hanson, G. R.; Gates, K. E.; Noble, C. J.; Griffin, M.; Mitchell, A.; Benson, S. *J. Inorg. Biochem.* **2004**, *98*, 903−916.

NOTE ADDED AFTER ASAP PUBLICATION

The paper was published ASAP on November 22, 2011 without the authors corrections. The corrected version reposted December 9, 2011.